2020

Hypoxia protects rat bone marrow mesenchymal stem cells against compression-induced apoptosis in the degenerative disc microenvironment through activation of the HIF-1a/YAP signaling pathway

Zhe Wang
Huazhong University of Science and Technology

Min Cui
Huazhong University of Science and Technology

Yanji Qu
Huazhong University of Science and Technology

Ruijun He
Washington University School of Medicine in St. Louis

Wei Wu
Huazhong University of Science and Technology

See next page for additional authors

STEM CELLS AND DEVELOPMENT
Volume 29, Number 20, 2020

DOI: 10.1089/scd.2020.0061

Hypoxia Protects Rat Bone Marrow Mesenchymal Stem Cells Against Compression-Induced Apoptosis in the Degenerative Disc Microenvironment Through Activation of the HIF-1α/YAP Signaling Pathway

Zhe Wang,[1] Min Cui,[1] Yanji Qu,[2] Ruijun He,[3] Wei Wu,[1] Hui Lin,[1] and Zengwu Shao[1]

Stem cell therapy provides an attractive solution for intervertebral disc (IVD) degeneration. However, the degenerative microenvironment, characterized by excessive mechanical loading and hypoxia, remains an obstacle for the long-lasting survival of exogenous transplanted stem cells. Whether and how bone marrow mesenchymal stem cells (BMSCs) adapt to the hostile microenvironment remain unclear. In this study, $CoCl_2$ and mechanical compression were simultaneously used to simulate the hypoxic and overloaded microenvironment of IVDs in vitro. Compression had a proapoptotic effect through activation of the mitochondrial apoptotic pathway, while hypoxia exerted a prosurvival effect counteracting compression-induced apoptosis. Inhibiting the transcriptional activity of hypoxia inducible factor 1 subunit alpha (HIF-1α) by chetomin reversed the antiapoptotic effect of hypoxia. Furthermore, HIF-1α promoted dephosphorylation and activation of yes-associated protein (YAP) in hypoxic conditions. Conversely, both YAP inhibition and increased cell apoptosis were observed after inhibition through chetomin or YAP inhibitor verteporfin. Immunofluorescence staining and coimmunoprecipitation assays revealed that YAP could interact directly with HIF-1α and colocalize in the nucleus. Taken together, our results demonstrated that hypoxia protected BMSCs against compression-induced apoptosis in the degenerative disc microenvironment through activation of the HIF-1α/YAP signaling pathway. Thus, regulation of HIF-1α/YAP signaling might provide novel insights for promoting long-lasting BMSC survival and optimizing stem cell therapy for IVD degeneration.

Keywords: intervertebral disc degeneration, bone marrow mesenchymal stem cells, hypoxia, apoptosis, HIF-1α, YAP

Introduction

Intervertebral disc degeneration (IVDD) is the primary cause of chronic low back pain, leading to patient disability and heavy social burden worldwide [1,2]. Stem cell therapy-based approaches offer an attractive solution for IVDD [3,4]. In particular, bone marrow mesenchymal stem cells (BMSCs) are recognized as excellent graft cells for intervertebral disc (IVD) regeneration due to their self-renewal capacity, multilineage differentiation potential, anti-inflammatory properties, and nonimmunogenic nature [5,6]. Numerous studies using autologous BMSCs for intradiscal transplantation to treat IVD degenerative diseases have shown encouraging outcomes, including improvements in the LBP score, retention of hydration in IVDs, and discogenic pain reduction in animal models and clinical trials [7–9]. However, the longest reported survival time of transplanted BMSCs in the degenerative disc was 8 months [10]. Recent studies have shown the existence of stem/progenitor cells within the IVD, suggestive of good prospects for endogenous IVD repair [11–14]. Despite promising preclinical results of stem cell therapy for IVDD, the challenge of the harsh microenvironment, which may not support the long-lasting survival of transplanted cells, remains [15].

During the course of IVDD, excessive mechanical loading, hypoxia, acidic conditions, and nutrient deprivation create a hostile microenvironment for resident cells while also compromising the regenerative efficacy of transplanted

Departments of [1]Orthopaedics and [2]Otorhinolaryngology, Union Hospital, Tongji Medical College, Huazhong University of Science and Technology, Wuhan, China
[3]Department of Developmental Biology, Washington University School of Medicine, St. Louis, Missouri, USA.

cells [4]. In particular, excessive mechanical loading has been considered a central contributor to extracellular matrix (ECM) degradation, intrinsic cell death, and IVDD initiation [16]. Accordingly, excessive compression may also challenge the survival of transplanted cells [17,18]. Cells transplanted into the avascular IVD have to adapt to the low-oxygen environment [5]. In hypoxic conditions, transplanted BMSCs maintain stemness, exhibit higher migration capacity, and are more resistant to apoptosis [19,20]. Hypoxia inducible factor 1 subunit alpha (HIF-1α) is the major transcriptional factor that activates the adaptive cellular response to hypoxia [21]. Previous studies have revealed the essential role of HIF-1α in cell survival and matrix synthesis in the nucleus pulposus (NP) [21,22]. Therefore, it is worthwhile to investigate the role of HIF-1α on transplanted BMSCs in hypoxia and compression.

Yes-associated protein (YAP) is a transcriptional coactivator in the Hippo signaling pathway. It plays prominent roles in tissue homeostasis, repair, and regeneration through regulation of stem cell proliferation and apoptosis [23–25]. Dephosphorylation and nuclear localization of YAP are required for its activation. Subsequently, YAP interacts with several DNA-binding transcription factors to induce the expression of target genes that control cell fate [26,27]. Recent studies have revealed the role of YAP dysregulation in progression of IVDD [28,29]. In addition, hypoxic cell survival is closely related to activation of YAP and its antiapoptotic target genes [30]. Therefore, YAP activation may be involved in hypoxic regulation of BMSCs under compression.

The aim of the current study was to investigate the effect of hypoxia on BMSCs under compression and the underlying regulatory mechanism. We reported the essential role of HIF-1α, which through its interaction with YAP in the nucleus, promoted BMSC survival in a degenerative disc microenvironment. Our findings might offer new directions for optimizing stem cell-based therapy for IVDD.

Materials and Methods

Cell isolation and culture

The experimental procedures were approved by the Animal Experimentation Committee of Tongji Medical College and conformed to the Guide for the Care and Use of Laboratory Animals. Rat BMSCs were isolated from 8-week-old female Sprague-Dawley rats as described previously with some modifications [31]. Briefly, BMSCs were collected by flushing the bone marrow with a sterile syringe from femurs of rats after sacrifice. The bone marrow was suspended in growth medium containing DMEM/F12 medium (Gibco) supplemented with 10% fetal bovine serum (FBS; Gibco) and 1% penicillin–streptomycin (Gibco) and maintained in 25-cm^2 culture flasks at 37°C in a humidified atmosphere containing 5% CO_2. Complete medium was replaced every 2 days and cells in passage two were used for subsequent experiments.

Multilineage differentiation assay

To assess the multilineage differentiation potential of BMSCs, osteogenic, adipogenic, and chondrogenic differentiation was induced. Briefly, BMSCs were seeded on 24-well plates at 2×10^4 cells/cm^2 with complete medium. For osteogenic induction, BMSCs that reached 70% confluency were induced with the osteogenic differentiation medium (Cyagen). The medium was changed every other day, and calcium nodules were stained with Alizarin Red after 3 weeks of induction. For adipogenic induction, BMSCs that reached complete confluency were induced with adipogenic differential medium A (Cyagen) for 3 days and then maintained with adipogenic differential medium B (Cyagen) for 1 day. After 4 cycles, the cells were cultured with medium B for 6 days and lipid droplets were then stained with Oil Red O. For chondrogenic induction, BMSCs that reached 70% confluency were induced with the chondrogenic differentiation medium (Cyagen) containing 1% TGF-β3. The medium was changed every 3 days, and glycosaminoglycan was stained with Alcian Blue after 3 weeks of induction. The typical images were obtained with an inversion microscope (Olympus IX71, Japan).

Surface marker identification of BMSCs

The first passage BMSCs were suspended at 10^6 cells/mL in PBS and aliquoted into 200 μL per tube. Cells were incubated with a working solution of antibodies, mouse anti-CD105 (Abcam; ab11414), mouse anti-CD90 (BD; 554897), mouse anti-CD73 (BD; 551123), rabbit anti-CD34 (Abcam; ab81289), mouse anti-CD45 (BD; 740515), and rabbit anti-HLA-DR (Bioss, bs-1198R), at 37°C for 1 h. The labeled cells were rinsed and then marked by secondary antibodies [Beyotime, A0562, FITC-labeled goat anti-rabbit IgG (H+L); Beyotime, A0568, FITC-labeled goat anti-mouse IgG (H+L)] at 37°C for 20 min. The unlabeled cells were analyzed in parallel. Cells were examined using flow cytometry with FACSCalibur (BD) following standard procedures.

Hypoxic culture and application of a compression apparatus

The compression apparatus, where cells were cultured inside, was an incubation chamber used to simulate the load on human lumbar discs, as we previously described [18,32–34]. BMSCs seeded on cell culture plates were placed into the chamber and then exposed to 1.0 MPa mechanical compression for 12, 24, 36, and 48 h. The whole apparatus was placed into a thermotank at 37°C. Besides, the concentration of CO_2 was maintained at 5%, monitored by a CO_2 indicator. Control cells were cultured in the absence of compression under the same culture conditions.

Cobalt chloride ($CoCl_2$; Sigma, United Kingdom) is a widely acknowledged chemical inducer of hypoxia. BMSCs were cultured in fresh complete medium, treated with different concentrations of $CoCl_2$ (0, 1, 10, 30, 50, 100, and 200 μM), and then exposed to compression for 12, 24, 36, and 48 h. The control group (0 μM) was cultured in the absence of compression under the same culture conditions. Additionally, the HIF-1α inhibitor chetomin (CHT, Selleck) and YAP inhibitor verteporfin (VP, MCE) were applied to cells 1 h before hypoxic culture, respectively.

Cell viability assay

Cell viability was measured using the cell counting kit-8 (CCK-8, Dojindo, Japan), following the manufacturer's instructions. BMSCs were seeded at a density of 5×10^3 cells/well

into 96-well plates. After exposure to compression and $CoCl_2$ with different concentrations for 12, 24, 36, and 48 h, 90 μL of medium and 10 μL of CCK-8 solution were added to each well and the plate was maintained at 37°C for 2 h in the dark. The optical density (OD) values at 450 nm were measured using a spectrophotometer (BioTek).

Annexin V/PI staining

The apoptosis rate of BMSCs was determined using an Annexin V-FITC Apoptosis Detection Kit (KeyGen Biotech, China). After treatment, cells were harvested by trypsinization, washed twice in PBS, and resuspended in 200 μL of binding buffer. Next, 5 μL of Annexin V and 5 μL of PI were added to the suspensions and subsequently analyzed by flow cytometry (BD LSR II), and data were analyzed using FlowJo, V10, software. The apoptosis rate was calculated as the sum of early apoptotic (Annexin V+ PI-) cells and late apoptotic (Annexin V+ PI+) cells.

Mitochondrial membrane potential assay

Mitochondrial membrane potential (MMP) was measured with the JC-1 fluorescent probe (Beyotime, China). Cells were incubated with a 500 μL working solution for 20 min at 37°C. After rinsing twice with precooling buffer solution, cells were resuspended in medium and analyzed by flow cytometry. Mitochondria with higher potential were labeled with red fluorescence produced by JC-1 aggregates. The lower potential mitochondria, which indicated an early stage of apoptosis, were labeled with green fluorescence produced by JC-1 monomers. The MMP was expressed as the ratio of red fluorescence intensity to green fluorescence intensity.

TUNEL staining

Apoptotic cells were detected using the One Step TUNEL Apoptosis Assay Kit (Beyotime, China). After incubating with the TUNEL reagent in the dark for 1 h at 37°C, cells were stained with 4′,6-diamidino-2-phenylindole (DAPI, Solarbio, China) for 5 min. Apoptotic cells showed red fluorescence (Cy3 labeled). Images of multiple cells from three independent experiments were obtained with a fluorescence inversion microscope (Olympus, Japan).

Western blot analysis

After treatments, the total protein of BMSCs was extracted by RIPA buffer (Beyotime, #P0013D, China) containing 1% phenylmethanesulfonyl fluoride (PMSF,

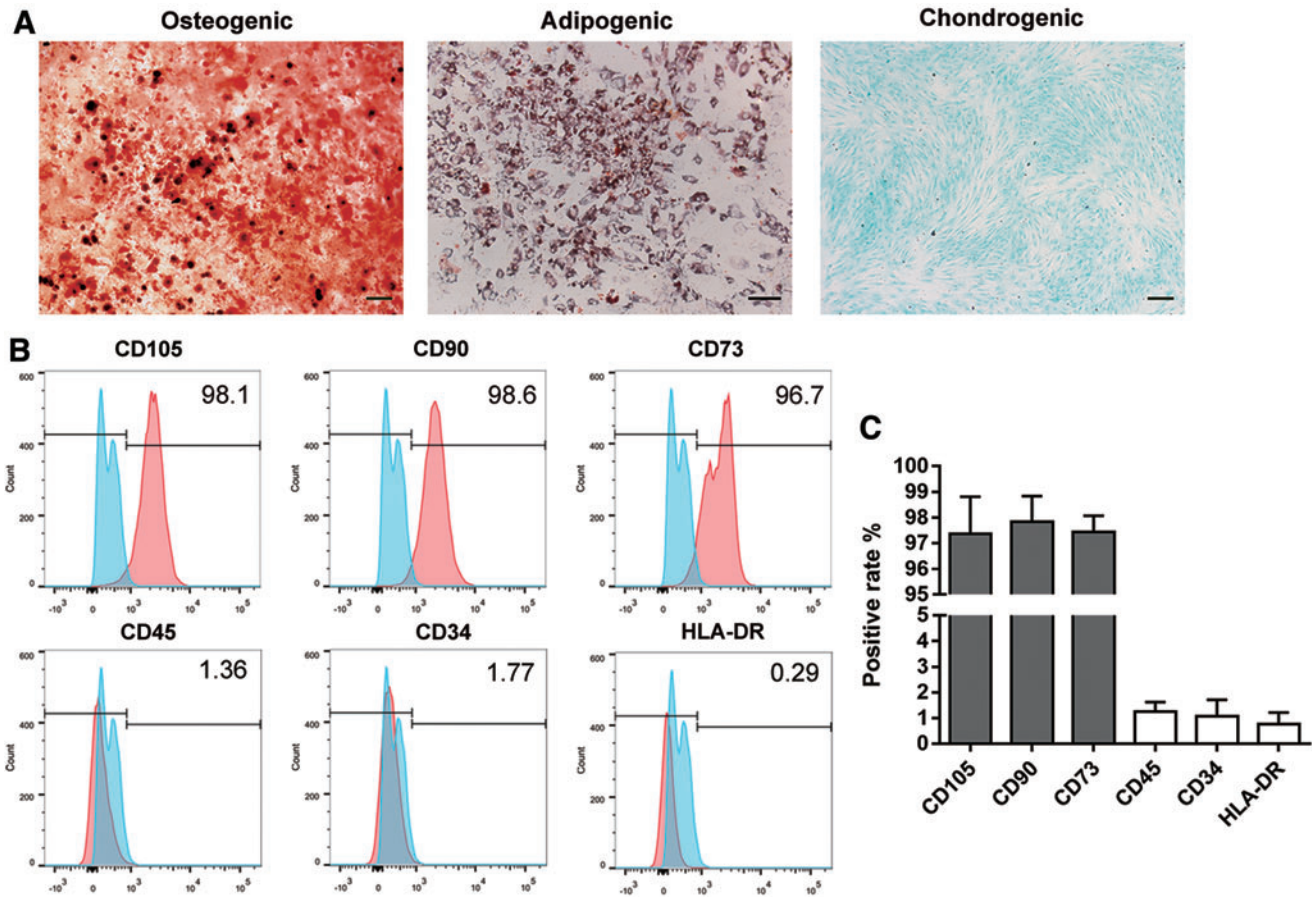

FIG. 1. Identification of BMSCs. **(A)** Alizarin Red, Oil Red O, and Alcian Blue staining were used to detect the osteogenic, adipogenic, and chondrogenic differentiation potential of BMSCs. Scale bar, 200 μm. **(B)** Surface markers of first passage BMSCs were detected by flow cytometry. *Red curves* indicate the percentage of labeled BMSCs and *blue curves* represent the blank control. **(C)** Positive rates of CD105, CD90, CD73, CD45, CD34, and HLA-DR, results are shown as mean ± SD. BMSC, bone marrow mesenchymal stem cell. Color images are available online.

Beyotime, China) and phosphorylase inhibitor (Servicebio, China). Protein concentration was determined using a BCA protein assay kit (Beyotime). Then, cell lysates were separated by SDS-PAGE (Beyotime) and transferred to PVDF membranes (Millipore). Blots were incubated overnight at 4°C with the following primary antibodies: HIF-1α (1:500, Novus, NB100-105), caspase-3 (1:1000, Proteintech, 19677-1-AP), Bcl-2 (1:1000, Abcam, ab196495), Bax (1:1000, CST, #2772), YAP (1:1000, CST, #14074), p-YAP Ser127 (1:1000, CST, #13008), and β-actin (1:1000, CST, #3700). Immunoblotting was detected using the UVP ChemiDoc-It Imaging System and enhanced chemiluminescence detection kit (Affinity; KF003).

Immunofluorescence

Cells cultured in six-well plates were rinsed three times with phosphate-buffered saline (PBS) and fixed in 4% polyformaldehyde for 15 min. After permeabilization with 0.5% Triton X-100 for 10 min, cells were blocked with 0.1% BSA for 30 min at room temperature. The cells were incubated with the primary antibody (HIF-1α, 1:200, Novus, NB100-105) overnight at 4°C. After rinsing, cells were incubated with Cy3-conjugated goat anti-mouse IgG (H+L) (1:100, Boster, BA1031) for 1 h at room temperature. Following rinsing with PBS, cells were blocked with 0.1% BSA again and incubated with the primary antibody (YAP, 1:200, CST, #14074) and the secondary antibody FITC-conjugated goat anti-rabbit IgG (H+L) (1:100, Boster, BA1105). We counterstained the cells using DAPI (Solarbio, C0065, China) and visualized them under a fluorescence microscope (Olympus, Japan).

Coimmunoprecipitation

Cells were lysed in RIPA buffer supplemented with 1% PMSF. Cell lysates were incubated with an equal amount of primary Rabbit anti-YAP antibody (5 μL, CST, #14074) or IgG at 4°C overnight before performing the pull-down assay with 20 μL of protein A + G agarose (Beyotime; #P2012) for 2 h. Beads were washed four times with lysis buffer, boiled, and the supernatant was subjected to SDS-PAGE and western blotting.

Statistical analysis

Statistical analysis was conducted using GraphPad Prism 7 software (GraphPad Software, Inc.). All data are presented as mean ± standard deviation (SD) from at least three independent experiments. Multiple sets of data were analyzed by one-way or two-way ANOVA, followed by Tukey's post hoc test. Student's *t* tests were performed to analyze the differences between two groups. Statistical significance was set at $P < 0.05$.

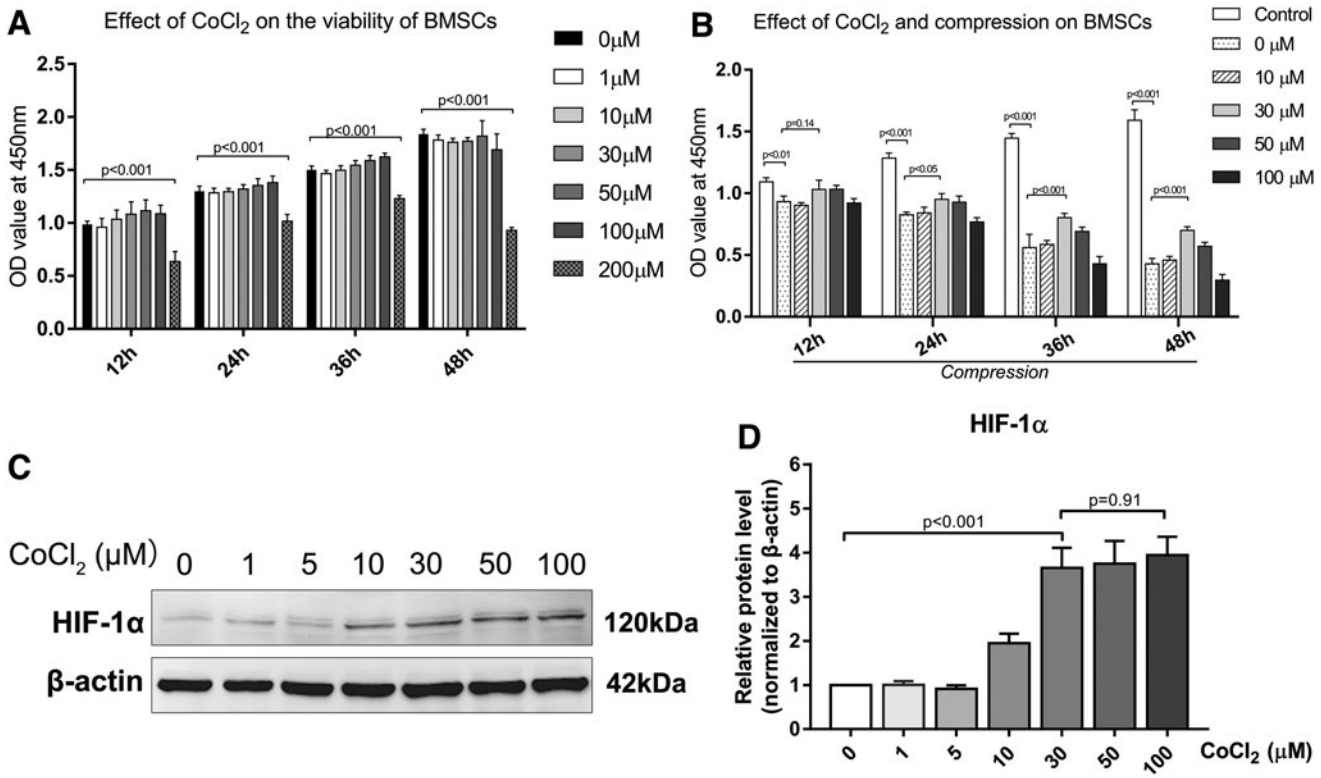

FIG. 2. The effect of $CoCl_2$ and compression on BMSC viability. **(A)** The CCK-8 assay was used to detect the cytotoxicity of $CoCl_2$ for different concentrations on BMSCs. **(B)** The cell viability of BMSCs treated with compression and different concentrations of $CoCl_2$ for 12, 24, 36, and 48 h was detected. Results are shown as mean ± SD. *P* values are labeled in numbers in the statistical chart. **(C)** Western blot analysis assessed the hypoxic simulation effect of $CoCl_2$ with different concentrations for 48 h. β-Actin served as the internal control. **(D)** Densitometric analysis of the relative HIF-1α level is shown in the statistical chart (normalized to 0 μM, $CoCl_2$ group). Results are shown as mean ± SD and *P* values are indicated in numbers in the statistical chart.

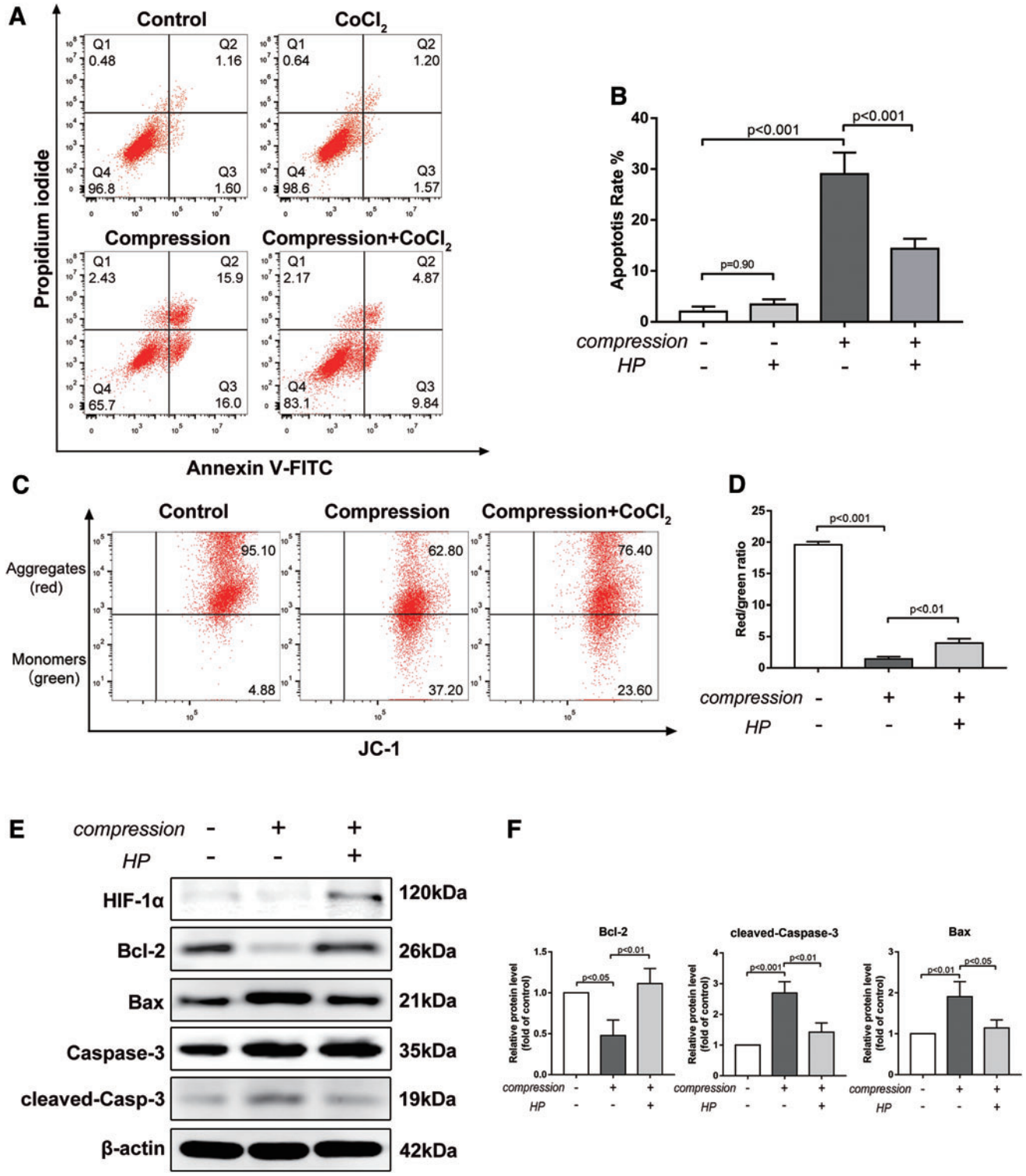

FIG. 3. $CoCl_2$-simulated hypoxia alleviated compression-induced BMSC apoptosis. **(A)** Flow cytometry analysis of Annexin V/PI double staining was used to detect the apoptosis rate of BMSCs treated with 48-h compression and 30 μM $CoCl_2$. **(B)** Quantitative analysis of the apoptosis rate is shown as mean ± SD. *P* values are indicated in numbers in the statistical chart. HP, hypoxia. **(C)** JC-1 staining was used to detect MMP changes in BMSCs by flow cytometry. The MMP level is expressed as the ratio of *red* fluorescence intensity (JC-1 aggregates) to *green* fluorescence intensity (JC-1 monomers). **(D)** Quantitative analysis of the *red/green* ratio is shown in the statistical chart. **(E)** Western blot analysis of HIF-1α and apoptosis-related proteins in BMSCs treated with compression and HP. **(F)** Densitometric analysis of the relative apoptosis-related protein level (normalized to the control group). Results are shown as mean ± SD and *P* values are indicated in numbers in the statistical chart. MMP, mitochondrial membrane potential; HIF-1α, hypoxia inducible factor 1 subunit alpha. Color images are available online.

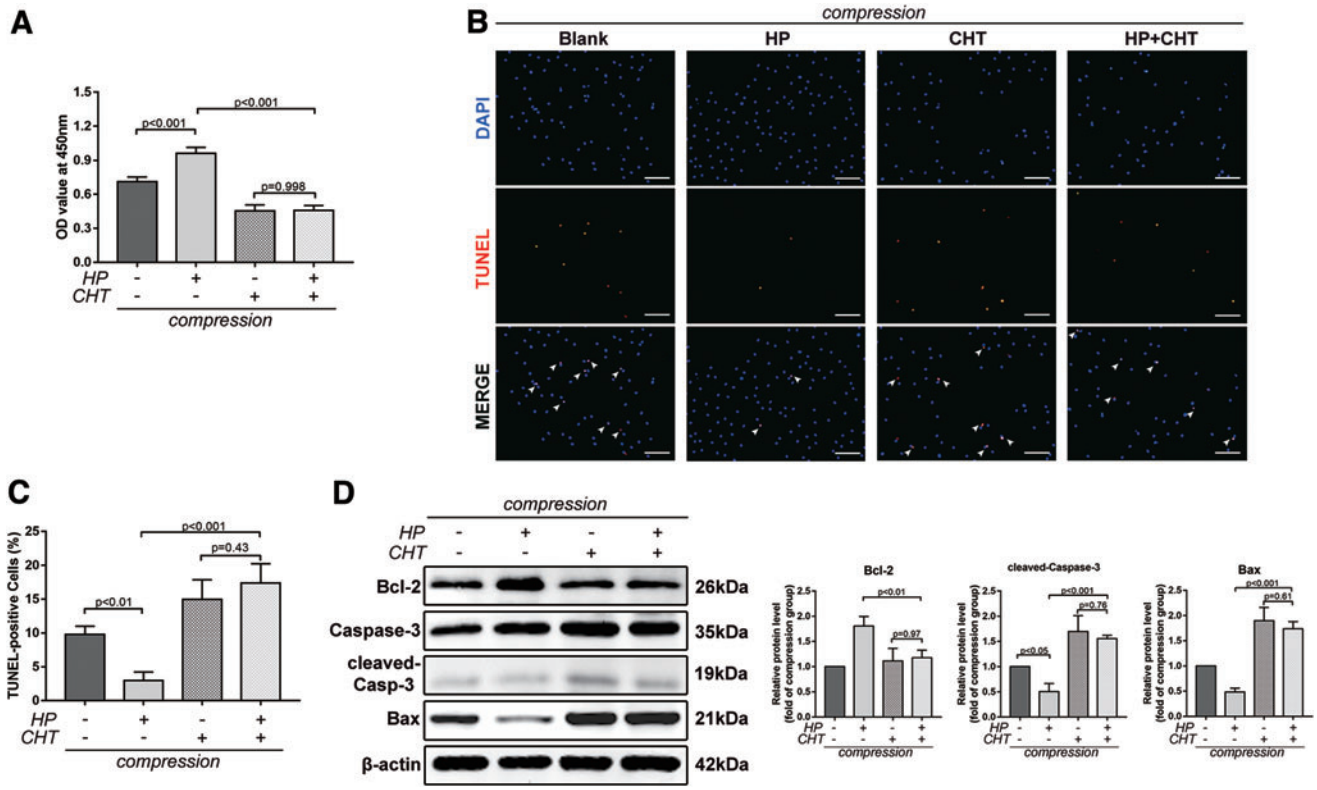

FIG. 4. HIF-1α mediated the antiapoptotic effect of BMSCs under compression. **(A)** The CCK-8 assay was used to detect cell viability of BMSCs treated with CHT and HP under compression. **(B)** TUNEL staining (*red* signal) was used to detect apoptotic changes in BMSCs treated with CHT and HP under compression. The nucleus was labeled with DAPI. The *white arrowhead* indicates the TUNEL-positive cell. Scale bar, 200 μm. **(C)** Quantitative analysis of the TUNEL-positive rate is shown in the statistical chart. **(D)** Western blot analysis showed expression of apoptosis-related proteins in BMSCs treated with CHT and HP under compression. The densitometric analysis is shown in the statistical chart (normalized to the compression group). Results are shown as mean ± SD and *P* values are indicated in numbers in the statistical chart. CCK-8, cell counting kit-8. Color images are available online.

Results

Identification of BMSCs

The isolated BMSCs could be effectively induced into osteogenic, adipogenic, and chondrogenic differentiation, respectively (Fig. 1A). Meanwhile, flow cytometric analysis showed that BMSCs expressed stem cell markers, including CD73, CD90, and CD105 (positive rate >95%), and were negative for CD34, CD45, and HLA-DR (positive rate <2%) (Fig. 1B, C).

Effect of $CoCl_2$ and compression on BMSC viability

$CoCl_2$ suppresses prolyl hydroxylation and pVHL-mediated degradation of HIF-1α, thus stabilizing the expression of HIF-1α and simulating hypoxic conditions [35]. $CoCl_2$ showed no significant cytotoxicity up to 100 μM on BMSCs (Fig. 2A). To establish the overloaded and hypoxic microenvironment of IVDs in vitro, cells were exposed to various concentrations of $CoCl_2$ and 1.0 MPa compression for 12, 24, 36, and 48 h. The CCK-8 assay was performed to determine the effect of compression and hypoxia on viability of BMSCs. Cell viability decreased significantly under compression in a time-dependent manner. Treatment with 30 μM $CoCl_2$ reversed the inhibitory effect of compression on cell viability, which was most apparent at 48 h ($P < 0.001$) (Fig. 2B). In addition, the expression level of HIF-1α at 48 h was detected to explore the simulation effect of $CoCl_2$ on BMSCs. Our data indicated that HIF-1α exhibited a notably altered and stable expression pattern with 30 μM $CoCl_2$ as the minimum effective concentration (Fig. 2C, D).

FIG. 5. Hypoxia exerted protective effects through activation of the HIF-1α/YAP signaling pathway. **(A)** Western blot analysis showed expression levels of YAP and p-YAP with CHT treatment under compression and hypoxia. **(B)** The densitometric analysis of the relative ratio p-YAP/YAP is shown in the statistical chart (normalized to the compression group). Results are shown as mean ± SD. **(C)** Western blot analysis of HIF-1α, YAP, p-YAP, Bax, and cleaved caspase-3 with VP treatment under compression and hypoxia. **(D)** The densitometric analysis is shown in the statistical chart. **(E)** Immunofluorescence staining of HIF-1α (*red*) and YAP (*green*) in BMSCs treated with VP under compression and hypoxia. The nucleus is labeled with DAPI. Scale bar, 20 μm. **(F)** Co-IP assay of endogenous YAP and HIF-1α in BMSCs under hypoxia and compression. YAP, yes-associated protein. Color images are available online.

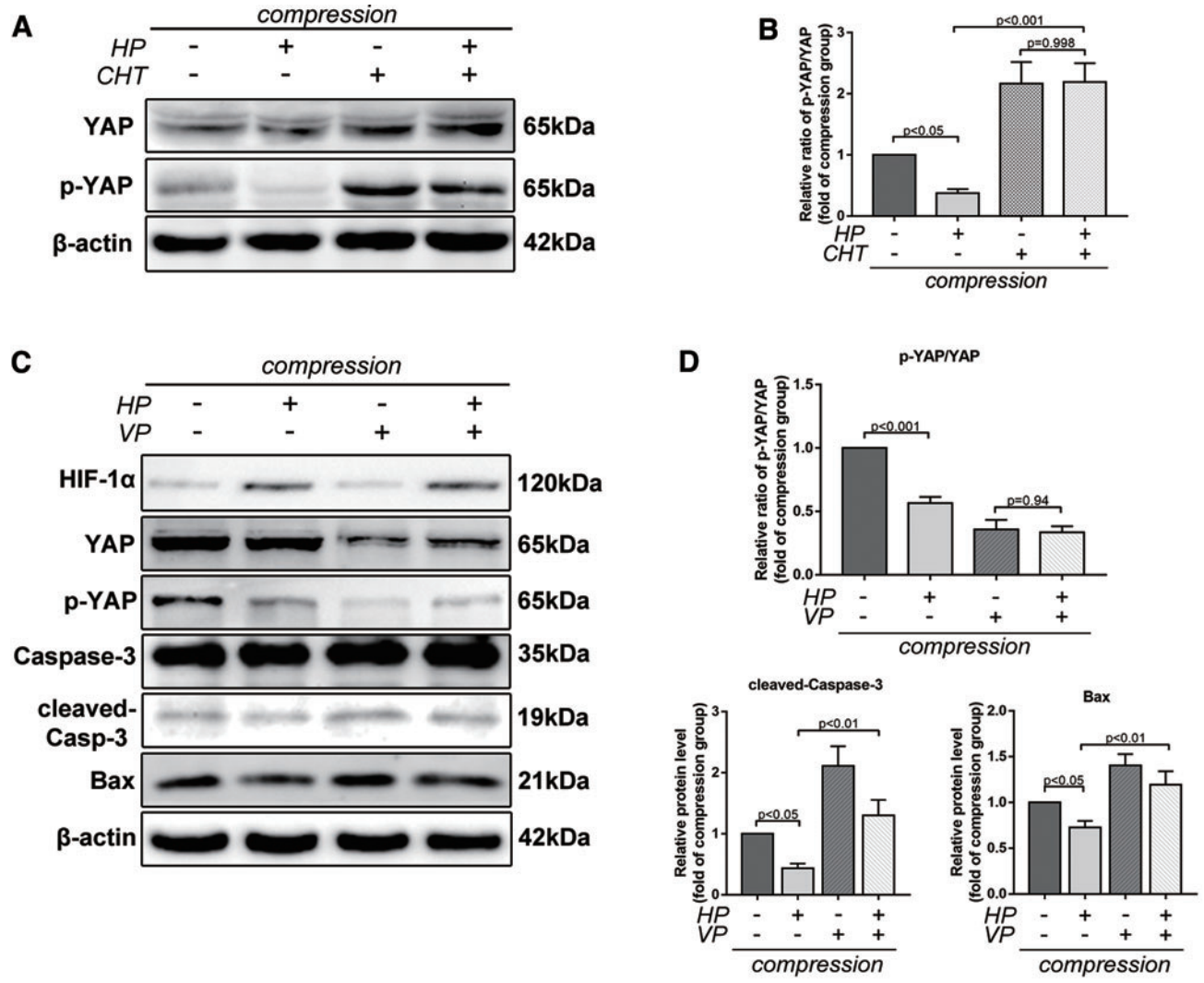

$CoCl_2$-simulated hypoxia alleviated compression-induced BMSC apoptosis

The Annexin V/PI apoptosis assay showed that 48-h compression significantly increased the apoptosis rate compared with the control group. However, $CoCl_2$-simulated hypoxia (HP) alleviated the apoptosis rate of BMSCs compared with the compression group (14.36% ± 1.60% in the compression+HP group vs. 29.02% ± 3.45% in the compression group, $P < 0.001$) (Fig. 3A, B). To further explore the effect of HP and compression on BMSC apoptosis, MMP was detected with a fluorescent probe, JC-1. MMP loss reflects mitochondrial dysfunction and is generally perceived as an early sign of apoptosis. MMP loss was observed in the compression group, as indicated by the decreased red/green fluorescence ratio, while HP restored compression-induced MMP loss ($P < 0.01$) (Fig. 3C, D). Western blot results showed that the antiapoptosis protein, Bcl-2, was downregulated, while the proapoptosis proteins, Bax and cleaved caspase-3, increased under compression. However, the mitochondrial apoptotic pathway was significantly inhibited by HP (Fig. 3E, F). These results showed that HP alleviated compression-induced BMSC apoptosis through the mitochondrial apoptotic pathway.

HIF-1α mediated the antiapoptotic effect of BMSCs under compression

To investigate whether the antiapoptotic effect was HIF-1α dependent, we used chetomin (CHT, 50 nM), a protein that inhibits the transcriptional activity of HIF-1α. CHT disrupts the structure of the CH1 domain of p300 coactivator, which precludes its interaction with the C-terminal transactivation domain of HIF-1α, inhibiting hypoxia inducible transcription activation [36]. Cell viability decreased remarkably with the CHT treatment, and no significant difference was observed between CHT and HP+CHT groups (Fig. 4A). Moreover, CHT blocked the antiapoptotic effect of HP under compression, indicated by the elevated TUNEL-positive rate (17.41% ± 2.45% in the HP+CHT group vs. 2.99% ± 1.07% in the HP group under compression, $P < 0.001$) and increased brightly stained condensed nuclei (Fig. 4B, C). Increased protein levels of Bax and cleaved caspase-3, along with a decreased level of Bcl-2, were observed in the presence of CHT (Fig. 4D). In summary, these results demonstrated that the antiapoptotic effect of HP under compression was mediated by HIF-1α.

Hypoxia exerted protective effects through activation of the HIF-1α/YAP signaling pathway

YAP is crucial to stem cell survival in tissue regeneration. Thus, the association between HIF-1α and YAP and their roles in protecting BMSCs against compression-induced apoptosis were investigated. Both p-YAP (Ser127) and the ratio of p-YAP/YAP reduced in hypoxia, while increased accumulation of p-YAP was observed when CHT was applied. It implied that hypoxia-induced YAP activation was dependent on the transcriptional activity of HIF-1α (Fig. 5A, B). We used verteporfin (VP, 10 nM), an FDA-approved YAP-selective inhibitor, to inhibit the expression of YAP and disturb the interaction between YAP and several DNA-binding transcription factors [37,38]. VP treatment decreased both YAP and p-YAP expression. Meanwhile, VP abrogated the antiapoptotic effect of hypoxia and upregulated the expression of proapoptotic proteins, which demonstrated the essential role of YAP in compression-induced apoptosis (Fig. 5C, D). Taken together, these results revealed that hypoxia exerted protective effects on BMSCs under compression through activation of the HIF-1α/YAP signaling pathway.

Considering that YAP nuclear translocation is the key regulatory mechanism for YAP activation, we performed immunofluorescence staining to examine the interaction and localization of HIF-1α and YAP in hypoxia and compression. HIF-1α and YAP were both activated and colocalized in the nucleus under hypoxia, while YAP maintained cytoplasmic retention and phosphorylated under compression without hypoxia. Additionally, VP blocked YAP from translocating into the nucleus in hypoxia (Fig. 5E). As a transcriptional coactivator, YAP was activated by and colocalized with HIF-1α. Thus, we further speculated that YAP could bind to HIF-1α in hypoxia. Coimmunoprecipitation (Co-IP) assay confirmed that YAP could directly interact with HIF-1α (Fig. 5F). Thus, HIF-1α recruited and bound to YAP in hypoxia, thereby forming a complex in the nucleus and transactivating target genes responsible for cellular survival (Fig. 6).

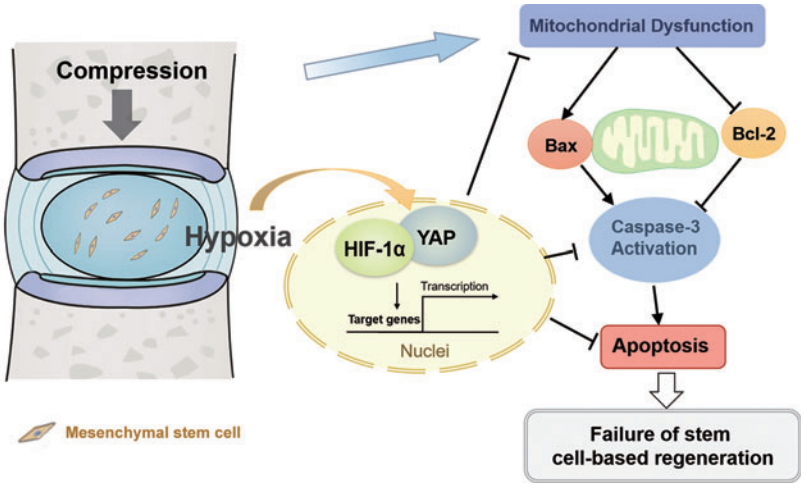

FIG. 6. The schematic diagram shows the effect of a hypoxic and overloaded disc microenvironment on transplanted bone marrow mesenchymal stem cells for IVD regeneration. In hypoxia, HIF-1α recruits and binds to YAP, thereby forming a complex in the nucleus and transactivating target genes responsible for cellular survival. IVD, intervertebral disc. Color images are available online.

Discussion

In the current study, we evaluated the effects of hypoxia and compression on BMSCs and investigated the mechanism underlying these effects. Importantly, hypoxia could protect BMSCs against compression-induced apoptosis through inhibition of the mitochondrial apoptotic pathway. Our research revealed that the antiapoptotic effect of hypoxia was mediated by HIF-1α. As hypoxia triggered YAP activation, we hypothesized that HIF-1α recruited and bound to YAP in the nucleus, inducing the expression of target genes responsible for cell survival.

Major advances have been made in stem cell therapy for IVDD [39]. However, the degenerative disc microenvironment, mainly characterized by excessive mechanical loading and hypoxia, remains an obstacle for the long-lasting survival of transplanted mesenchymal stem cells. In particular, excessive mechanical loading plays a crucial role in the progression of IVDD [40]. Previous studies have shown the proapoptotic effects of compression on NP cells and NP progenitor/stem cells [18,32]. Similarly, our results showed that compression not only reduced BMSC viability but also induced apoptosis through the mitochondrial apoptotic pathway [18]. Furthermore, we found that hypoxia could alleviate compression-induced apoptosis by reducing MMP loss and restoring mitochondrial function. These results suggested that hypoxia was beneficial for transplanted BMSC survival. Cells that reside in the hypoxic niche of healthy IVDs of mammals showed stable expression of HIF-1α [41]. It has been previously demonstrated that HIF-1α played a vital role in cell survival and ECM homeostasis during IVDD [21]. In our in vitro experiment, the control group and compression group were exposed to normoxic conditions. In the presence of oxygen, HIF-1α was degraded through the proteasome and prolyl hydroxylases in an oxygen-dependent manner [42], which resulted in a nonsignificant effect of compression alone on HIF-1α levels.

Under hypoxic conditions, HIF-1α is stabilized and accumulates in the nucleus where it triggers transcriptional activation [43]. Under CHT stimuli, the reduced cell viability and increased TUNEL-positive rate were not reversed by HP treatment, indicating that the antiapoptotic effect was dependent on the transcriptional activity of HIF-1α. Moreover, CHT reversed the inhibitory effect of HP on the mitochondrial apoptotic pathway. Thus, we confirmed that the antiapoptotic effect of hypoxia was mediated by HIF-1α. Previous studies have also shown that hypoxic mesenchymal stem cells exhibited a high capacity for ECM synthesis and high migration ability, both of which are also HIF-1α dependent [44,45]. Additionally, neovascularization with increased oxygen concentration may occur in severely degenerated discs [46], which may contribute to the compromised efficacy of stem cell therapy in patients with severe disc degeneration.

In the present study, we demonstrated that hypoxia promoted BMSC survival under compression by upregulating YAP expression and triggering its nuclear translocation. CHT treatment blocked hypoxia-induced YAP recruitment into the nucleus and its activation, which implied that YAP activation was mediated by HIF-1α. VP disrupted the activity of YAP as a transcriptional coactivator and promoted YAP degradation, along with elevated proapoptotic protein levels, suggesting that YAP activation was essential for the prosurvival effect of hypoxia. As a transcriptional coactivator, YAP was activated by and colocalized with HIF-1α. A co-IP assay revealed that YAP could bind to HIF-1α under compression and hypoxic conditions. Taken together, HIF-1α recruits and binds to YAP in hypoxia, thereby forming a complex in the nucleus and transactivating target genes responsible for cellular survival. However, the specific target genes activated by the HIF-1α/YAP complex require further study.

In conclusion, our study demonstrated the protective effect of hypoxia against compression-induced apoptosis of BMSCs through activation of HIF-1α/YAP signaling and revealed the adaptive mechanism of BMSCs to hypoxia in a degenerative disc microenvironment. Further studies should explore the long-term survival of transplanted BMSCs overexpressing HIF-1α or YAP in animal models. Meanwhile, the target genes upregulated by the HIF-1α/YAP complex require further investigation. Future preclinical trials and animal experiments using HIF-1α- or YAP-overexpressing BMSCs for intradiscal injection may provide a therapeutic strategy for optimizing stem cell therapy in IVDD treatment.

Author Disclosure Statement

No competing financial interests exist.

Funding Information

This study was supported by grants (91649204) from the Major Research Plan of the National Natural Science Foundation of China and the Scientific Research Training Program for Young Talents in Union Hospital, Tongji Medical College, Huazhong University of Science and Technology, China.

References

1. Luoma K, H Riihimäki, R Luukkonen, R Raininko, E Viikari-Juntura and A Lamminen. (2000). Low back pain in relation to lumbar disc degeneration. Spine (Phila Pa 1976) 25:487–492.
2. Paige NM, IM Miake-Lye, MS Booth, JM Beroes, AS Mardian, P Dougherty, R Branson, B Tang, SC Morton and PG Shekelle. (2017). Association of spinal manipulative therapy with clinical benefit and harm for acute low-back pain systematic review and meta-Analysis. JAMA 317:1451–1460.
3. Sakai D and S Grad. (2015). Advancing the cellular and molecular therapy for intervertebral disc disease. Adv Drug Deliv Rev 84:159–171.
4. Wang F, R Shi, F Cai, YT Wang and XT Wu. (2015). Stem Cell Approaches to Intervertebral Disc Regeneration: obstacles from the Disc Microenvironment. Stem Cells Dev 24:2479–2495.
5. Huang YC, VYL Leung, WW Lu and KDK Luk. (2013). The effects of microenvironment in mesenchymal stem cell-based regeneration of intervertebral disc. Spine J 13: 352–362.
6. Richardson SM, JA Hoyland, R Mobasheri, C Csaki, M Shakibaei and A Mobasheri. (2010). Mesenchymal stem cells in regenerative medicine: opportunities and

challenges for articular cartilage and intervertebral disc tissue engineering. J Cell Physiol 222:23–32.
7. Urits I, A Capuco, M Sharma, AD Kaye, O Viswanath, EM Cornett and V Orhurhu. (2019). Stem cell therapies for treatment of discogenic low back pain: a comprehensive review. Curr Pain Headache Rep 23:65.
8. Pettine KA, MB Murphy, RK Suzuki and TT Sand. (2015). Percutaneous injection of autologous bone marrow concentrate cells significantly reduces lumbar discogenic pain through 12 months. Stem Cells 33:146–156.
9. Centeno C, J Markle, E Dodson, I Stemper, CJ Williams, M Hyzy, T Ichim and M Freeman. (2017). Treatment of lumbar degenerative disc disease-associated radicular pain with culture-expanded autologous mesenchymal stem cells: a pilot study on safety and efficacy. J Transl Med 15:197.
10. Henriksson HB, N Papadimitriou, D Hingert, A Baranto, A Lindahl and H Brisby. (2019). The traceability of mesenchymal stromal cells after injection into degenerated discs in patients with low back pain. Stem Cells Dev 28:1203–1211.
11. Blanco JF, IF Graciani, FM Sanchez-Guijo, S Muntión, P Hernandez-Campo, C Santamaria, S Carrancio, MV Barbado, G Cruz, et al. (2010). Isolation and characterization of mesenchymal stromal cells from human degenerated nucleus pulposus: comparison with bone marrow mesenchymal stromal cells from the same subjects. Spine (Phila Pa 1976) 35:2259–2265.
12. Brisby H, N Papadimitriou, C Brantsing, P Bergh, A Lindahl and H Barreto Henriksson. (2013). The presence of local mesenchymal progenitor cells in human degenerated intervertebral discs and possibilities to influence these in vitro: a descriptive study in humans. Stem Cells Dev 22:804–814.
13. Henriksson HB, M Thornemo, C Karlsson, O Hägg, K Junevik, A Lindahl and H Brisby. (2009). Identification of cell proliferation zones, progenitor cells and a potential stem cell niche in the intervertebral disc region: a study in four species. Spine (Phila Pa 1976) 34:2278–2287.
14. Risbud MV, A Guttapalli, TT Tsai, JY Lee, KG Danielson, AR Vaccaro, TJ Albert, Z Gazit, D Gazit and IM Shapiro. (2007). Evidence for skeletal progenitor cells in the degenerate human intervertebral disc. Spine (Phila Pa 1976) 32:2537–2544.
15. Sakai D and GBJ Andersson. (2015). Stem cell therapy for intervertebral disc regeneration: obstacles and solutions. Nat Rev Rheumatol 11:243–256.
16. Yurube T, H Hirata, K Kakutani, K Maeno, T Takada, Z Zhang, K Takayama, T Matsushita, R Kuroda, M Kurosaka and K Nishida. (2014). Notochordal cell disappearance and modes of apoptotic cell death in a rat tail static compression-induced disc degeneration model. Arthritis Res Ther 16:1–11.
17. Ma K, S Chen, Z Li, X Deng, D Huang, L Xiong and Z Shao. (2019). Mechanisms of endogenous repair failure during intervertebral disc degeneration. Osteoarthr Cartil 27:41–48.
18. Ding F, ZW Shao, SH Yang, Q Wu, F Gao and LM Xiong. (2012). Role of mitochondrial pathway in compression-induced apoptosis of nucleus pulposus cells. Apoptosis 17: 579–590.
19. Lin M, X Liu, H Zheng, X Huang, Y Wu, A Huang, H Zhu, Y Hu, W Mai and Y Huang. (2020). IGF-1 enhances BMSC viability, migration, and anti-apoptosis in myocardial infarction via secreted frizzled-related protein 2 pathway. Stem Cell Res Ther 11:22.
20. Han Y-S, JH Lee, YM Yoon, CW Yun, H Noh and SH Lee. (2016). Hypoxia-induced expression of cellular prion protein improves the therapeutic potential of mesenchymal stem cells. Cell Death Dis 7:e2395.
21. Merceron C, L Mangiavini, A Robling, TL Wilson, AJ Giaccia, IM Shapiro, E Schipani and MV Risbud. (2014). Loss of HIF-1α in the notochord results in cell death and complete disappearance of the nucleus pulposus. PLoS One 9:e110768.
22. Liu Z, C Li, X Meng, Y Bai, J Qi, J Wang, Q Zhou, W Zhang and X Zhang. (2017). Hypoxia-inducible factor-lα mediates aggrecan and collagen Π expression via NOTCH1 signaling in nucleus pulposus cells during intervertebral disc degeneration. Biochem Biophys Res Commun 488:554–561.
23. Tremblay AM and FD Camargo. (2012). Hippo signaling in mammalian stem cells. Semin Cell Dev Biol 23:818–826.
24. Yu FX, B Zhao and KL Guan. (2015). Hippo Pathway in Organ Size Control, Tissue Homeostasis, and Cancer. Cell 163:811–828.
25. Moya IM and G Halder. (2019). Hippo–YAP/TAZ signalling in organ regeneration and regenerative medicine. Nat Rev Mol Cell Biol 20:211–226.
26. Pan D. (2010). The hippo signaling pathway in development and cancer. Dev Cell 19:491–505.
27. Deng Y, J Lu, W Li, A Wu, X Zhang, W Tong, KK Ho, L Qin, H Song and KK Mak. (2018). Reciprocal inhibition of YAP/TAZ and NF-κB regulates osteoarthritic cartilage degradation. Nat Commun 9:4564.
28. Zhang C, F Wang, Z Xie, L Chen, A Sinkemani, H Yu, K Wang, L Mao and X Wu. (2018). Dysregulation of YAP by the Hippo pathway is involved in intervertebral disc degeneration, cell contact inhibition, and cell senescence. Oncotarget 9:2175–2192.
29. Zhang C, F Wang, Z Xie, L Chen, A Sinkemani, H Yu and X Wu. (2018). AMOT130 linking F-actin to YAP is involved in intervertebral disc degeneration. Cell Prolif 51: 1–12.
30. Greenhough A, C Bagley, KJ Heesom, DB Gurevich, D Gay, M Bond, TJ Collard, C Paraskeva, P Martin, et al. (2018). Cancer cell adaptation to hypoxia involves a HIF-GPRC5A-YAP axis. EMBO Mol Med 10:e8699.
31. Tu C, Y Xiao, Y Ma, H Wu and M Song. (2018). The legacy effects of electromagnetic fields on bone marrow mesenchymal stem cell self-renewal and multiple differentiation potential. Stem Cell Res Ther 9:1–11.
32. Hu Y, L Huang, M Shen, Y Liu, G Liu, Y Wu, F Ding, K Ma, W Wang, et al. (2019). Pioglitazone protects compression-mediated apoptosis in nucleus pulposus mesenchymal stem cells by suppressing oxidative stress. Oxid Med Cell Longev 2019:1–30.
33. Lin H, L Zhao, X Ma, BC Wang, XY Deng, M Cui, SF Chen and ZW Shao. (2017). Drp1 mediates compression-induced programmed necrosis of rat nucleus pulposus cells by promoting mitochondrial translocation of p53 and nuclear translocation of AIF. Biochem Biophys Res Commun 487:181–188.
34. Ma KG, ZW Shao, SH Yang, J Wang, BC Wang, LM Xiong, Q Wu and SF Chen. (2013). Autophagy is activated in compression-induced cell degeneration and is mediated by reactive oxygen species in nucleus pulposus cells exposed to compression. Osteoarthr Cartil 21:2030–2038.
35. Schofield CJ and PJ Ratcliffe. (2004). Oxygen sensing by HIF hydroxylases. Nat Rev Mol Cell Biol 5:343–354.

36. Viziteu E, C Grandmougin, H Goldschmidt, A Seckinger, D Hose, B Klein and J Moreaux. (2016). Chetomin, targeting HIF-1α/p300 complex, exhibits antitumour activity in multiple myeloma. Br J Cancer 114:519–523.
37. Gibault F, F Bailly, M Corvaisier, M Coevoet, G Huet, P Melnyk and P Cotelle. (2017). Molecular Features of the YAP Inhibitor Verteporfin: synthesis of Hexasubstituted Dipyrrins as Potential Inhibitors of YAP/TAZ, the Downstream Effectors of the Hippo Pathway. ChemMedChem 12:954–961.
38. Liu-Chittenden Y, B Huang, JS Shim, Q Chen, SJ Lee, RA Anders, JO Liu and D Pan. (2012). Genetic and pharmacological disruption of the TEAD-YAP complex suppresses the oncogenic activity of YAP. Genes Dev 26: 1300–1305.
39. Clouet J, M Fusellier, A Camus, C Le Visage and J Guicheux. (2019). Intervertebral disc regeneration: from cell therapy to the development of novel bioinspired endogenous repair strategies. Adv Drug Deliv Rev 146:306–324.
40. Kuo YJ, LC Wu, JS Sun, MH Chen, MG Sun and YH Tsuang. (2014). Mechanical stress-induced apoptosis of nucleus pulposus cells: an in vitro and in vivo rat model. J Orthop Sci 19:313–322.
41. Pan H, A Strickland, V Madhu, ZI Johnson, SN Chand, JR Brody, A Fertala, Z Zheng, IM Shapiro and MV Risbud. (2019). RNA binding protein HuR regulates extracellular matrix gene expression and pH homeostasis independent of controlling HIF-1α signaling in nucleus pulposus cells. Matrix Biol 77:23–40.
42. Cook KM, N Kataria, CA Martinez, B Kerr, SS Zaiter, M Morgan and SR McAlpine. (2019). C-terminal HSP90 inhibitors block the HIF-1 hypoxic response by degrading HIF-1α through the oxygen-dependent degradation pathway. Cell Physiol Biochem 53:480–495.
43. Li H, CZ Liang and QX Chen. (2013). Regulatory role of hypoxia inducible factor in the biological behavior of nucleus pulposus cells. Yonsei Med J 54:807–812.
44. Wang W, Y Wang, G Deng, J Ma, X Huang, J Yu, Y Xi and X Ye. (2018). Transplantation of hypoxic-preconditioned bone mesenchymal stem cells retards intervertebral disc degeneration via enhancing implanted cell survival and migration in rats. Stem Cells Int 2018: 7564159.
45. Chiang ER, HL Ma, JP Wang, MC Chang, CL Liu, TH Chen and SC Hung. (2019). Use of Allogeneic Hypoxic Mesenchymal Stem Cells For Treating Disc Degeneration in Rabbits. J Orthop Res 37:1440–1450.
46. Pai RR, B D'sa, CV Raghuveer and A Kamath. (1999). Neovascularization of nucleus pulposus: a diagnostic feature of intervertebral disc prolapse. Spine (Phila Pa 1976) 24:739–741.

Address correspondence to:
Dr. Min Cui
Department of Orthopaedics
Union Hospital
Tongji Medical College
Huazhong University of Science and Technology
1277 Jiefang Avenue
Wuhan 430022
China

E-mail: cm95588@hust.edu.cn

Received for publication March 24, 2020
Accepted after revision August 14, 2020
Prepublished on Liebert Instant Online August 16, 2020